

Improving estimates of brain connectivity in autism spectrum disorder

Benjamin Risk

Department of Biostatistics and Bioinformatics, Emory University

thebrisklab.org



- 1 Accounting for motion in brain connectivity studies of autistic children
- 2 Sparse ICA with an Application to Cortical Surface fMRI Data
- 3 Brain Connectivity Across the Autism Spectrum Dataset

Introduction: Autism spectrum disorder

- 1 in 31 children in the US diagnosed with ASD (Shaw et al. 2025).
- Deficits in social communication and interaction; restricted and repetitive behaviors, interests, and activities.
- **Autism awareness video**

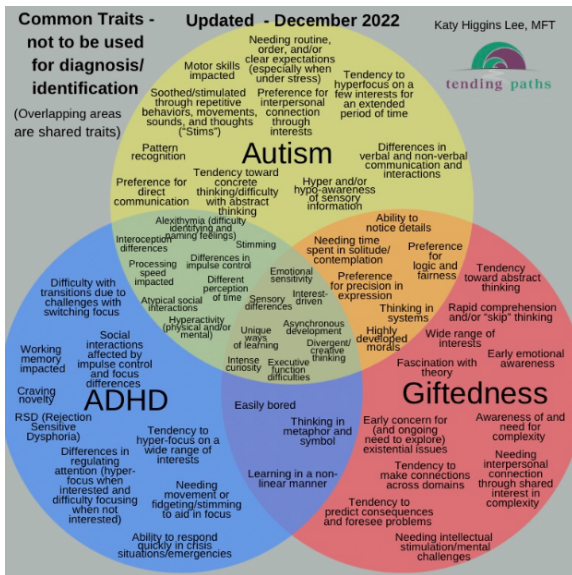


Understand autism and what you can do to help.

www.autism.org.uk



Introduction: Neurodiversity and neurodivergence



Autism Language Preferences

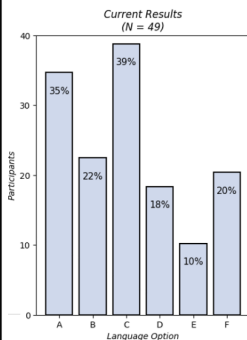
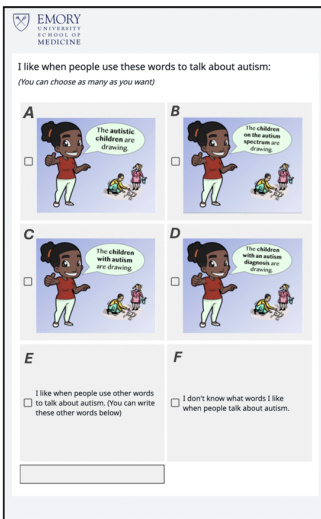


Figure: Survey of 8-13 year old children with autism designed by Jamie Kotanek.

Additional comments on terminology

Write-in comments included the following:

- Write-in preferred terms: neurospicy, specky, neurodivergent.
 - “I don’t like it when people describe me, it’s embarrassing.”
 - “I don’t mind when scientists talk about autism, but when random people do.”
 - “I don’t like when people talk about it. But only close friend and family can call me autistic.”

Brain connectivity and autism

- Autism is a neurodevelopmental disorder thought to be related to alterations in brain function.
- Resting-state fMRI is used to examine functional connectivity, or correlations between brain regions.
- Connectivity theory of autism:
 - Underconnectivity in long-range connections (Just et al. 2012).
 - Overconnectivity in local connections (Keown et al. 2013).
- Disruptions in the default mode network (Yerys et al. 2015), including anterior-to-posterior parts (Di Martino et al. 2013).
- Some similarities with the patterns produced by motion artifacts (Deen and Pelphrey 2012).

Default mode decreased connectivity

The intrinsic brain architecture in autism
A Di Martino et al

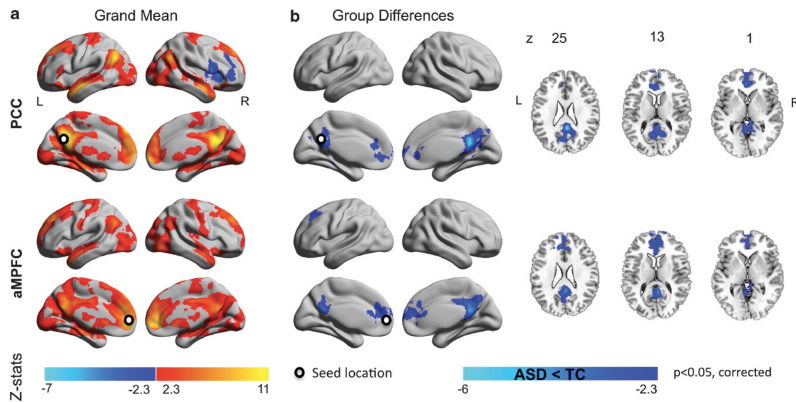
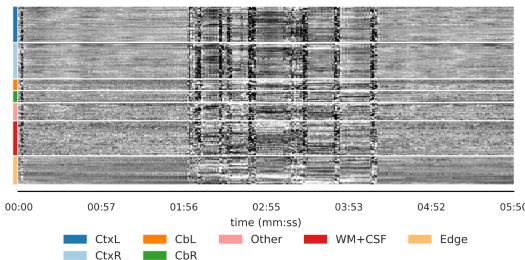


Figure: Di Martino et al. (2014)

Problem I: Motion Artifacts



Rigid body motion correction

Nuisance signals regression
(Ciric et al. 2017)

Remove scans with excessive motion
(Satterthwaite et al. 2013, Power 2017,
Parkes et al. 2018)

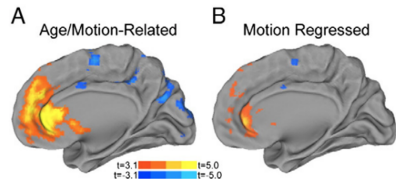
- Existing motion control using regression is inadequate because motion patterns are complex (Power et al. 2014).
- Current best practices remove time points with framewise displacement >0.2 mm, then remove participants if < 5 minutes of data remain after this scrubbing.

Challenges in pediatric neuroimaging

Motion challenges:

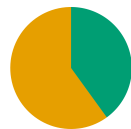
- Younger children move more (Satterthwaite et al. 2012)
- Confounding with neurodevelopmental trajectories.

"It really, really, really sucks. My favorite result of the last five years is an artifact." -*Steven Petersen, Professor of cognitive neuroscience at Washington University in St. Louis.*



Problem II: Motion QC creates selection bias

- State of the art: remove high motion participants.
- Motion control leads to drastic reductions in sample size.
- ABCD study **removed 60 – 75%** of children due to excessive motion (Marek et al. 2022, Nielsen et al. 2019).
- In ABCD, this creates selection bias, disproportionately selecting for: higher SES, White participants, older, females, higher neurocognitive skills, fewer neurodevelopmental problems (Cosgrove et al. 2022).
- Unethical?



Higher motion in autistic children in ABIDE

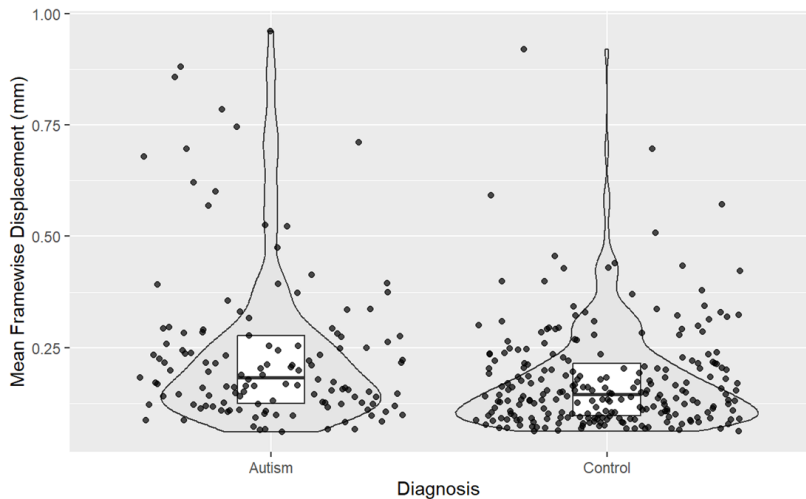


Figure: 8-13 year-olds from the ABIDE dataset.

Participant removal creates selection bias in ASD

M.B. Nebel, D.E. Lidstone, L. Wang et al.

NeuroImage 257 (2022) 119296

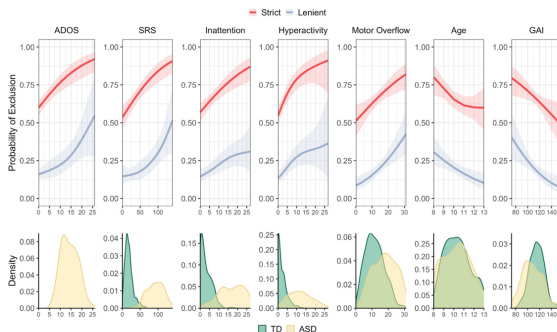


Fig. 4. rs-fMRI exclusion probability changes with phenotype and age. Univariate analysis of rs-fMRI exclusion probability as a function of participant characteristics. From left to right: Autism Diagnostic Observation Schedule (ADOS) total scores, social responsiveness scale (SRS) scores, inattentive symptoms, hyperactive/impulsive symptoms, total motor overflow, age, and general ability index (GAI) using the lenient (slate blue lines, all FDR-adjusted $p < 0.01$), and strict (red lines) motion quality control (all FDR-adjusted $p < 0.03$). Variable distributions for each diagnosis group (included and excluded scans) are displayed across the bottom panel (TD=typically developing, green; ASD=autism spectrum disorder, yellow).

Motion Control (MoCo) in Functional Connectivity Studies in Children with Autism Spectrum Disorder

Jialu Ran¹, Sarah Shultz², Benjamin Risk¹ and David Benkeser¹

¹*Department of Biostatistics and Bioinformatics*, ²*Department of Pediatrics, Emory University*



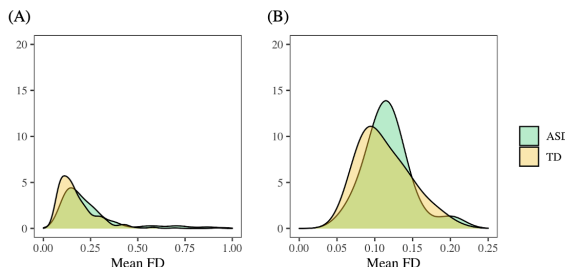
Stochastic Intervention

What would the autistic brain look like under low motion?

We use the framework of stochastic intervention (Díaz et al. 2021).

Replace **mean framewise displacement M** by tolerable value

$$M \sim P_{M|\Delta=1,A=0,X}$$



Motion-Controlled Estimand (MoCo)

Motion-Controlled Estimand (MoCo): the difference between the autistic and non-ASD brain when all children have a tolerable amount of motion.

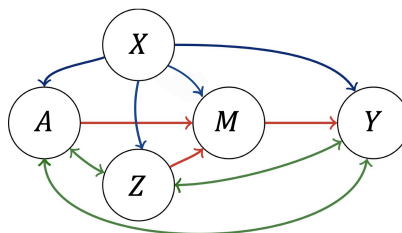
- A : non-ASD (0), ASD (1)
- M : a motion variable (mean framewise displacement)
- X : demographic variables.
- Z : variables related to autism symptoms.

$$\int \left[\{ \mu_{Y|A,M,X,Z}(1, m, x, z) p_{Z|A,X}(z|1, x) \right. \\ \left. - \mu_{Y|A,M,X,Z}(0, m, x, z) p_{Z|A,X}(z|0, x) \} \right. \\ \left. p_{M|\Delta=1,A,X}(m|0, x) p_X(x) \right] dz dm dx .$$

Intuition: estimating what brain looks like under the counterfactual of low motion.

Marginal estimand

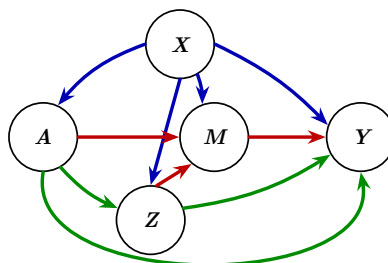
Our approach treats motion as a mediator:



- $Y \in \mathbb{R}$: functional connectivity between two locations in the brain
- $A \in \{0, 1\}$: non-ASD (0), ASD (1)
- $M \in \mathbb{R}$: a motion variable (mean framewise displacement)
- X : demographic variables (age, sex and handedness)
- Z : variables related to autism symptoms (autism diagnostic score, IQ, medication status)

Directed acyclic graph

Time-ordering of data implies the directional graph:



- $Y \in \mathbb{R}$: functional connectivity between two locations in the brain
- $A \in \{0, 1\}$: non-ASD (0), ASD (1)
- $M \in \mathbb{R}$: a motion variable (mean framewise displacement)
- X : demographic variables (age, sex and handedness)
- Z : variables related to autism symptoms

Estimation: one-step estimator

- We define a one-step estimator.
- Allows for **statistical inference with machine-learning**.
- Machine-learning of nuisance regressions:
 - Motion density estimation using highly adaptive lasso.
 - **SuperLearner** to learn conditional means and propensities: multivariate adaptive regression splines, LASSO, ridge regression, generalized additive models, generalized linear models, random forest, and xgboost.
- Cross-fitting for better type-1 control.
- Multiple robustness.
- Simultaneous confidence bands via the efficient influence function (family-wise error rate control).

Theorem (Efficient Influence Function)

Define

$$\pi_a(x) = P(A = a | X = x),$$

$$\bar{\pi}_0(x) = P(A = 0 | X = x)P(\Delta = 1 | A = 0, X = x),$$

$$r_a(m, x, z) = \frac{p_{M|\Delta=1,0,X}(m | x)}{p_{M|a,X,Z}(m | x, z)}.$$

The efficient influence function for θ_a is

$$\begin{aligned} D_{P,a}(O_i) &= \frac{\mathbf{1}_a(A_i)}{\pi_a(X_i)} r_a(M_i, X_i, Z_i) \{Y_i - \mu_{Y|a,M,X,Z}(M_i, X_i, Z_i)\} \\ &\quad + \frac{\mathbf{1}_a(A_i)}{\pi_a(X_i)} \{\eta_{\mu|a,Z,X}(X_i, Z_i) - \xi_{\eta|a,X}(X_i)\} \\ &\quad + \frac{\mathbf{1}_{a,1}(A_i, \Delta_i)}{\bar{\pi}_0(X_i)} \{\eta_{\mu|a,M,X}(M_i, X_i) - \xi_{\eta|a,X}(X_i)\} + \xi_{\eta|a,X}(X_i) - \theta_a. \end{aligned}$$

\sqrt{n} -Convergence

Theorem (Asymptotic normality)

Under the following assumptions,

- (i) Positivity of estimates: $\pi_{n,a} > \epsilon_1$ for some $\epsilon_1 > 0$, $\bar{\pi}_{n,0} > \epsilon_2$ for some $\epsilon_2 > 0$, and $\frac{p_{n,M|\Delta=1,0,X}}{p_{n,M|a,X,Z}} < \epsilon_3$ for some $\epsilon_3 < \infty$.
- (ii) $n^{1/2}$ -convergence of second order terms.
- (iii) $L^2(P)$ -consistent influence function estimate:

$$\int [\{ D_{a,P_\ell}(o) - D_{a,P_n}(o) \}^2] dP(o) = o_P(1),$$

where P_ℓ denotes the limit of P_n as $n \rightarrow \infty$.

- (iv) Donsker influence function estimate: D_{a,P_n} falls in a P -Donsker class with probability tending to 1.

Then,

$$\theta_{n,a}^+ - \theta_a = \frac{1}{n} \sum_{i=1}^n D_{a,P}(O_i) + o_P(n^{-1/2})$$

and

$$n^{1/2} (\theta_{n,a}^+ - \theta_a) \Rightarrow N(0, E[D_{P,a}(O)^2]).$$

Multiple robustness

	$\mu_{n,Y A,M,X,Z}$	$\eta_{n,\mu A,M,X}$	$\xi_{n,a,\eta X}$	$\bar{\pi}_{n,0}$	$\pi_{n,a}$	$p_{n,M \Delta=1,A,X}$	$p_{n,M A,X,Z}$
(B2.1)					✓	✓	✓
(B2.2)			✓			✓	✓
(B2.3)	✓	✓		✓	✓		
(B2.4)	✓				✓	✓	
(B2.5)	✓		✓			✓	

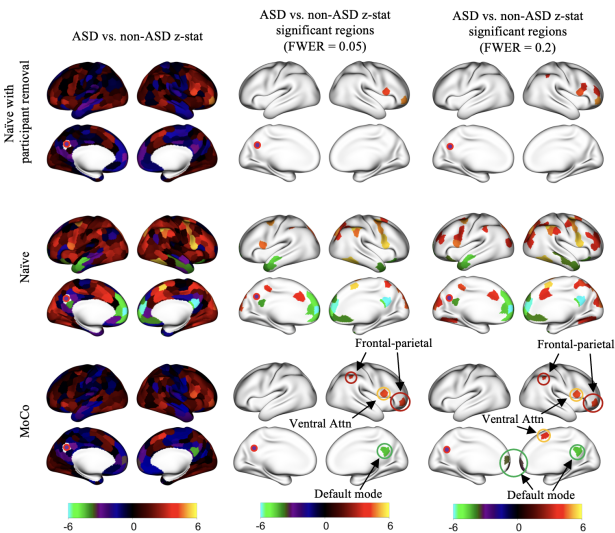
Table: Theorem: multiple robustness. Each row indicates a setting for consistency, where check marks indicate the nuisance parameters which, when they converge to true functions, then $E[D_{P',a}(O)] = 0$, and $\theta_{n,a}^+ \rightarrow \theta_a$. See Ran et al. (2024).

ABIDE Data

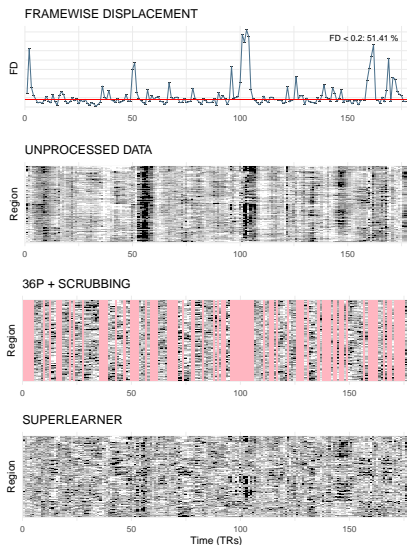
School-age children from Autism Brain Imaging Data Exchange (ABIDEI and ABIDEII) Dataset (Di Martino et al. 2014; 2017)

- variables:
 - A_i : 245 TD ($A = 0$), 132 ASD ($A = 1$) [377 8-13 yo children].
 - X_i : age, sex, handedness.
 - Z_i : autism diagnostic observation schedule, IQ, medication status.
 - M_i : mean frame-wise displacement (FD).
 - $\Delta_i = 1$: > 5 minutes of data free from ≥ 0.2 framewise displacement (Power et al. 2014) [126 TD (51%), 34 ASD (26%)].
- Y_{ij} : correlation between seed region in DMN and region j , $j = 1, \dots, 400$ (Schaaffer 400 atlas).
- SuperLearner for nuisance regressions: random forest, xgboost, multivariate adaptive regression splines, LASSO, ridge regression, generalized additive models, generalized linear models (with and without interactions, and with and without forward stepwise covariate selection)
- Highly adaptive lasso for conditional density estimation (Hejazi et al. 2022).
- Cross-fitting with 5-fold cross-validation.

ABIDE Inference



Future directions: time series correction



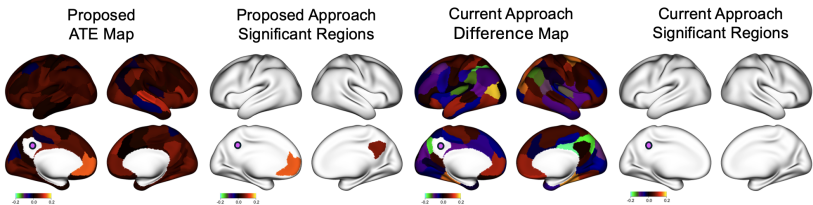


Figure: We have conducted a preliminary analysis using out-of-the-box super learner to remove motion artifacts in the time series of rs-fMRI in a study of autistic children, which demonstrates feasibility. Based on a seed region in the posterior default mode network (DMN) (fuchsia point), connectivity to the anterior DMN increased (FWER $p < 0.10$, approximate Cohen's $D = 0.85$). This effect was smaller and not significant when using 36p+scrubbing+removal.

Summary

- Our findings do not support the connectivity theory of autism.
- The decrease in long-range brain connectivity is partially due to motion artifacts.
- MoCo works with imperfectly cleaned correlations to perform additional motion correction.
- Uses ensemble of machine learning methods (random forests, multivariate adaptive regression splines, lasso, GAMs etc) to estimate nuisance regressions.
- Also uses highly adaptive lasso for estimating conditional motion densities.
- Reduces selection bias and improves statistical power.

Sparse Independent Component Analysis with an Application to Cortical Surface fMRI Data in Autism

Zihang Wang¹, Irina Gaynanova², Aleksandr Aravkin³ and
Benjamin Risk¹

¹*Department of Biostatistics and Bioinformatics, Emory University,*

²*Department of Biostatistics, University of Michigan,* ³*Department of Applied Mathematics, University of Washington*



Independent Component Analysis (ICA)

- Let $X \in \mathbb{R}^{P \times T}$ represent the fMRI time series for a single subject, where each column is a vectorized image of dimension P , and T is the number of time points.
- The noisy ICA model with isotropic noise is defined as

$$X = SM + N.$$

- $S \in \mathbb{R}^{P \times Q}$: matrix of non-Gaussian components (sources) with $Q < T$.
- $M \in \mathbb{R}^{Q \times T}$ is the mixing matrix.
- $N \in \mathbb{R}^{P \times T}$ is a matrix of normal random variables.

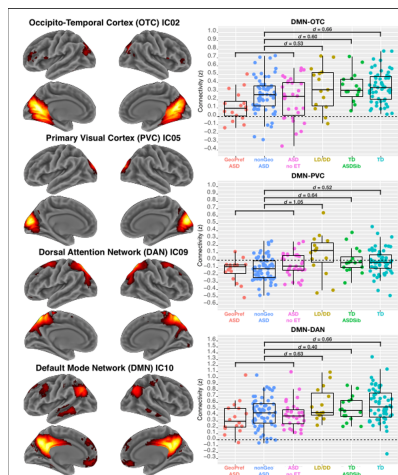
Background

- ICA is commonly applied to resting-state functional magnetic resonance imaging (fMRI) data (Smith et al. 2009).
- The independent components (ICs) are known as “resting-state networks,” which are sparse brain regions that tend to co-activate while the brain is not engaged in any tasks (Biswal et al. 2010).
- The correlations between the time courses of the components (functional connectivity) reveal brain communication patterns (Smith et al. 2015).
- Thresholding is commonly applied to components after estimation to aid visualization and interpretation (Smith et al. 2009).
- Subject-specific time courses are back reconstructed using the original unthresholded components (Calhoun et al. 2001).

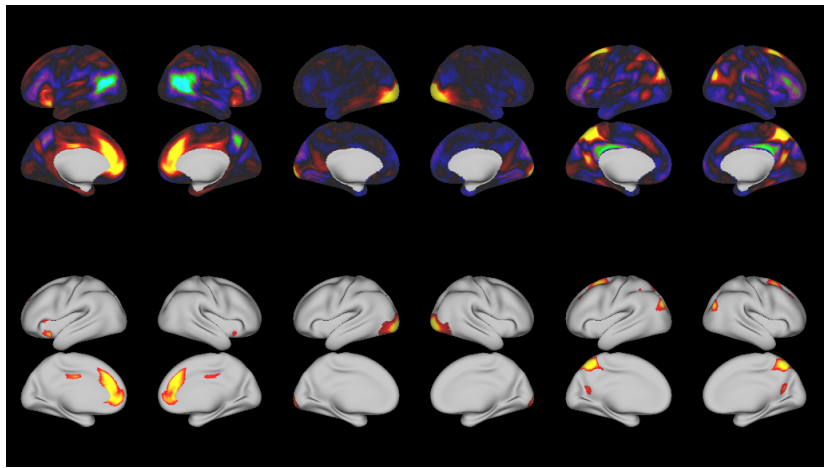
Toy example: ICA

Example Source Mixture

- ICA is popular in pediatric neuroimaging.
- Used as a study-specific brain atlas.
- Figure: Example application of ICA with post-hoc thresholding in a functional connectivity study of autism (Lombardo et al. 2019).



Thresholding is inaccurate



Previous methods

- Fast ICA and Infomax ICA are popular (Hyvarinen 1999, Bell and Sejnowski 1995): dense estimation.
- Sparse PCA (Zou et al. 2006, Shen and Huang 2008): independence is not enforced.
- Sparse Fast ICA (Ge et al. 2016): multiple tuning parameters, not exact sparsity.
- Sparse ICA entropy-bound minimization (SICA-EBM) (Boukouvalas et al. 2018): two tuning parameters, computationally costly, not exact sparsity.

Challenges

- ① Existing ICA algorithms are only capable of handling smooth objective functions.
- ② Solving the ICA problem involves non-convex optimization.
- ③ An ICA method should be fast for neuroimaging data.

Laplace ICA Model

- X is centered and whitened, $\tilde{X} \in \mathbb{R}^{P \times Q}$ such that $\tilde{X}^\top \tilde{X} = I_Q$, PCA+ICA used to approximate noisy ICA (Beckmann and Smith 2004):
- Let $U \in \mathcal{O}^{Q \times Q}$ be an orthogonal transformation.
- We aim to solve

$$\underset{U}{\text{minimize}} \quad J(\tilde{X}U) \quad \text{s.t.} \quad U^\top U = I_Q,$$

where

$$J(\tilde{X}U) = - \sum_{i=1}^P \sum_{j=1}^Q \log p_j \{(\tilde{X}U)_{ij}\} = - \sum_{i=1}^P \sum_{j=1}^Q \log p_j(\tilde{x}_i^\top u_j),$$

$p_j(s) = e^{-\frac{|s-\mu|}{\lambda}}/2\lambda$ be the density of a component, where $\mu = 0$ and $\lambda = \sqrt{2}/2$.

Relax-and-Split Framework

Algorithm challenges:

- Non-smooth objective function, can't use Newton-type algorithms like ICA fixed point algorithm.
- Orthogonality constraint on U , which is non-convex.

These challenges can be solved through the Relax-and-Split framework (Zheng and Aravkin 2020).

The relaxed problem

$$\underset{U,V}{\text{minimize}} \quad J(V) + \frac{1}{2\nu} \|V - \tilde{X}U\|_F^2 \quad \text{s.t.} \quad U^\top U = I_Q,$$

where the auxiliary V explicitly models the independent components S , and parameter ν controls the level of relaxation.

Alternating Updates

Algorithm 1 Relax and split ICA

- 1: **Input:** U^0, V^0
 - 2: Initialize: $k = 0$
 - 3: **while** not converged **do**
 - 4: $V^{k+1} \leftarrow \operatorname{argmin}_V J(V) + \frac{1}{2\gamma} \|V - \tilde{X}U^k\|_F^2$
 - 5: $U^{k+1} \leftarrow \operatorname{argmin}_{U^\top U=I} \|V^{k+1} - \tilde{X}U\|_F^2$
 - 6: $k \leftarrow k + 1$
 - 7: **Output:** U^k, V^k
-

It only requires two ingredients:

- Algorithm for V update: element-wise gradient descent.
- Algorithm for U update: orthogonal Procrustes problem.
- Repeat over a grid of ν with warm starts and select ν using a BIC-like criterion (Allen and Maletić-Savatić 2011).

Simulation Results: Components

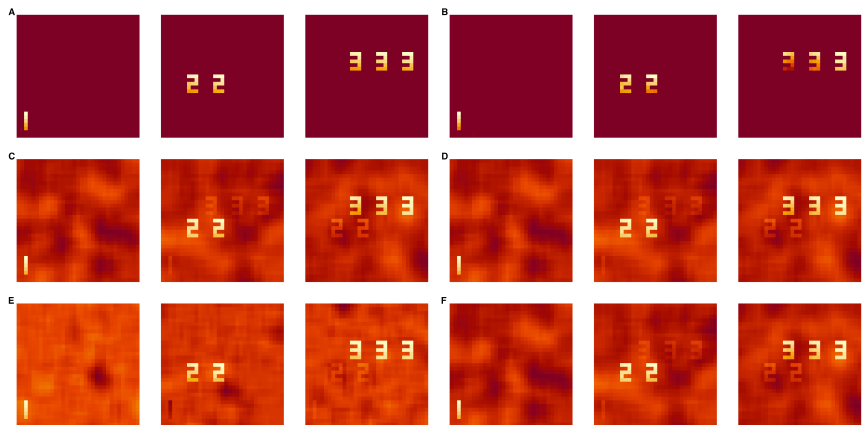
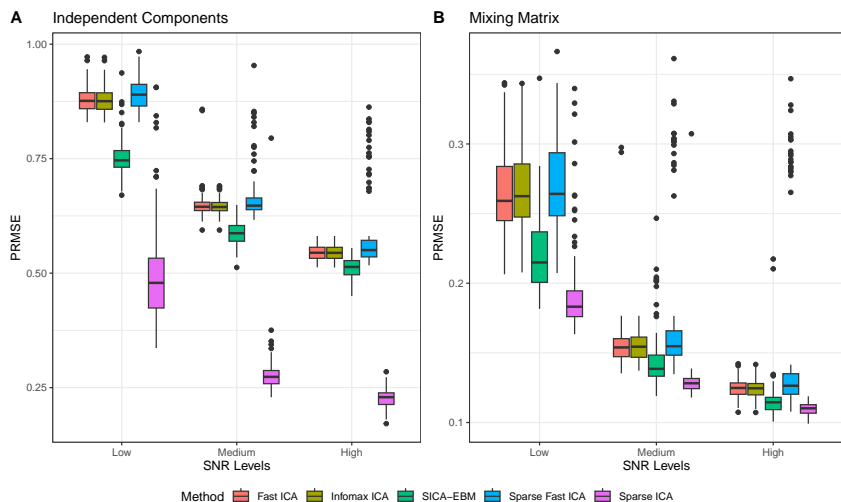


Figure: **A:** The true ICs. Zeros appear as maroon. **B:** Sparse ICA. **C:** Infomax ICA. **D:** Fast ICA. **E:** SICA-EBM. **F:** Sparse Fast ICA.

Simulation Results: Mixing matrix



Computation Time

	Sparse ICA	Fast ICA	Infomax ICA	SICA-EBM	Sparse Fast ICA
Low SNR	0.0080	0.0022	0.0141	16.0053	0.0055
Medium SNR	0.0079	0.0023	0.0186	22.9243	0.0024
High SNR	0.0081	0.0023	0.0177	19.9347	0.0019
High-dimensional	1.9147	0.4323	2.3359	2233.4951	0.0253

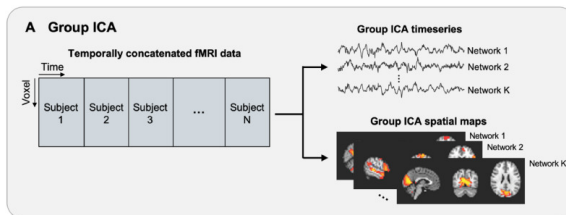
Table: Average computation times in seconds over 100 replications for Sparse ICA and other methods. SICA-EBM and Sparse Fast ICA are implemented in Matlab, other ICA methods are in R and RCpp.

Sparse ICA competitive, much faster than Infomax ICA and SICA-EBM.

ABIDE Study

- Applied Sparse ICA to the ABIDE study.
- 30 group components estimated.
- Subject-specific time courses were estimated to construct correlation matrices with the dimension of 30×30 .
- Account for selection bias from motion QC using augmented inverse probability of inclusion weighted estimation (Robins et al. 1994, Robins 2000), with SuperLearner for outcome and propensity models, follows Nebel et al. (2022).
- FDR-corrected p-values (Benjamini and Hochberg 1995).

Group ICA



Dual regression (stage 1)

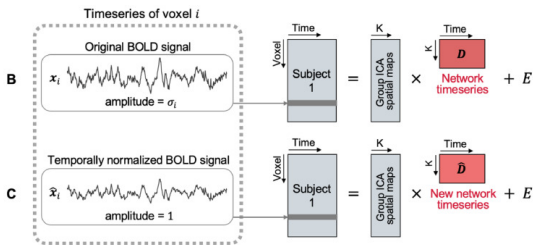


Figure: Taken from Lee et al. (2023).

Results

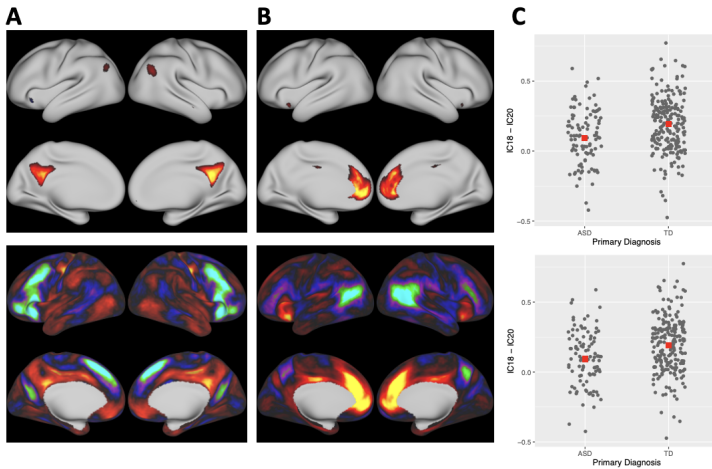


Figure: Panel A: medial posterior default mode network. **Panel B:** anterior part of the default mode network.

Results

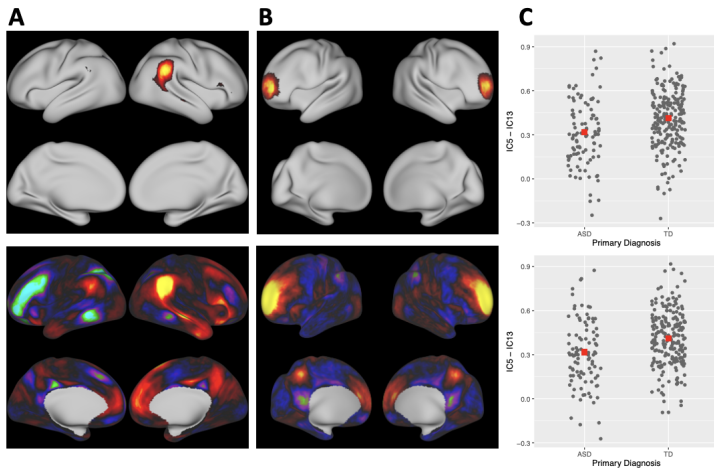


Figure: Panel A: temporal parietal junction. **Panel B:** frontoparietal network, associated with executive function

Summary

- A novel ICA method that estimates sparse independent components using a relax-and-split algorithm and is computationally fast.
- Sparse features improve interpretation and accuracy.
- Important for downstream functional connectivity analyses.
- In the real data application, we found:
 - decreased connectivity between the anterior and posterior parts of the default mode network in ASD versus non-ASD children.
 - decreased connectivity between executive function and control networks in ASD.

Paper and R Package

- Wang Z., Gaynanova, I., Aravkin, A., Risk, B. B. (2024). Sparse Independent Component Analysis with an Application to Cortical Surface fMRI Data in Autism. *Journal of the American Statistical Association*, 1–22.
- R package SparseICA available on:
<https://github.com/thebrisklab/SparseICA>.



Brain Connectivity Across the Autism Spectrum

Collaboration with Sarah Shultz,
Department of Pediatrics, Emory University School of Medicine
and the Marcus Autism Center



Limitations of previous studies

Previous studies have selection bias in *who* is in the study.

Exclusion criteria:

- Exclude children with intellectual disabilities.
- Exclude non-verbal children.
- Partly driven by site-specific limitations in feasibility.
- Limited training in a mock scanner.
- Children that can't complete a scan.

Brain Connectivity Across the Autism Spectrum

Aim: Characterize functional connectivity **across the autism spectrum** in school-age children (8-13 years old) through mock training combined with improved statistical methodology.

- Exclusion criteria: history of head trauma, seizure disorders, abnormality affecting visual or auditory acuity that cannot be corrected through eye-glasses or hearing aids, or any contraindication for MRI.
- No exclusion based on IQ. Non-verbal are not excluded.
- Experienced staff: Registered Behavior Technicians, Licensed Masters in Social Work, Licensed Associate Professional Counselor, Applied Behavior Analysis training.
- We exclude children exhibiting aggression that may be of harm to themselves or the study team.

Brain Connectivity Across the Autism Spectrum at Emory

- Multiple mock training sessions using MoTrak for motion feedback.
- FIRMM to monitor motion during MRI scan.
- Beneficial to families.
- brainconnectivitystudy.org



Figure: Top: MoTrak trains children to move less. FIRMM provides real-time motion feedback.

Reducing selection bias: study participants

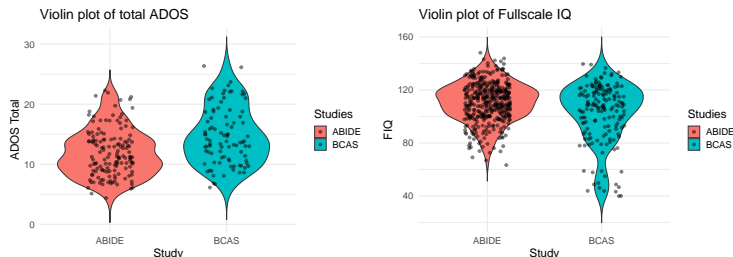


Figure: Comparison of the autism diagnostic observation schedule and full-scale IQ in the ABIDE study versus our study.

- Study sample is more representative of autistic children.
- Improved statistical methodology (MoCo and its extensions) allows us to use most of the data.

Motion is higher in autistic children: BCAS dataset

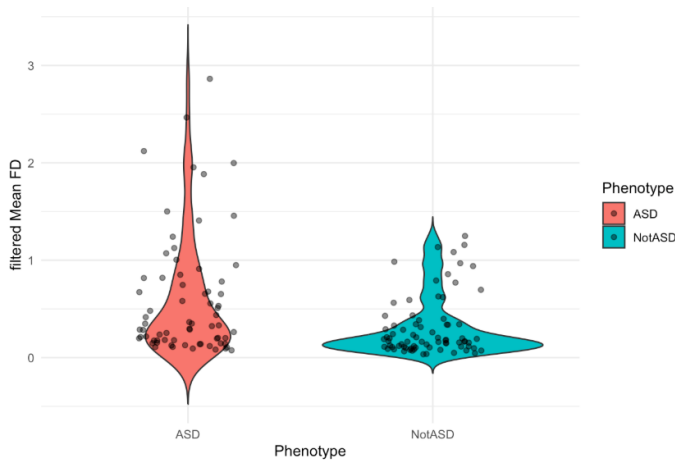
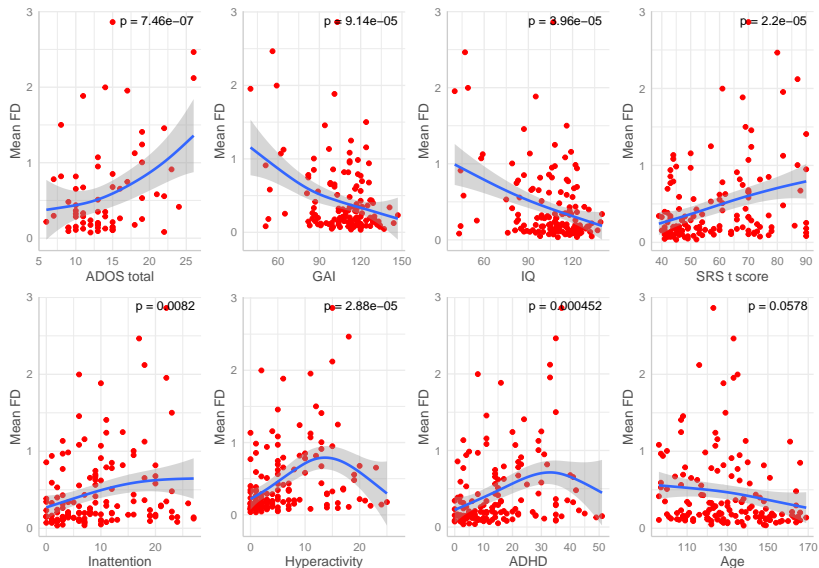


Figure: 8-13 year-olds from an ongoing study at Emory.

BCAS motion and behavioral measures



FastICA applied to BCAS

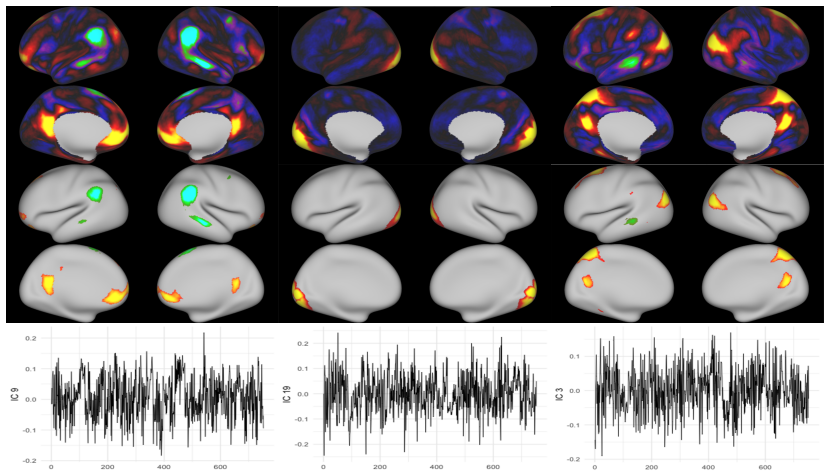


Figure: Group Fast ICA applied to 152 8-13 year old children and time courses from an example participant.

SparseICA applied to BCAS

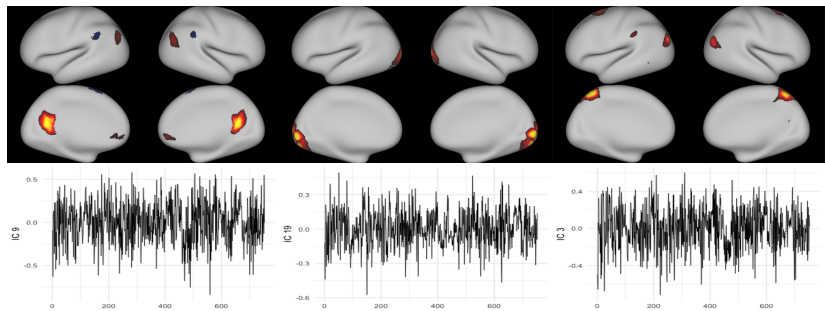


Figure: Group Sparse ICA applied to 152 8-13 year old children and time courses from an example participant.

Example of SparseICA+MoCo (draft)

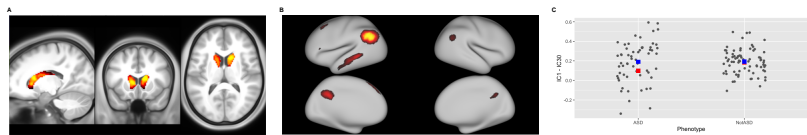


Figure: Preliminary results applying SparseICA+MoCo to the BCAS Dataset (75 ASD, 77 non-ASD). Example connection showing larger differences in MoCo compared to naive with participant removal.

Marcus Autism Center Team



Thank you!

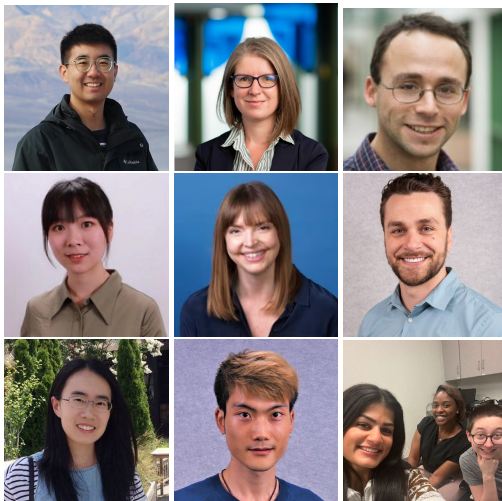


Figure: Zihang Wang (Emory), Irina Gaynanova (UM), Aleksandr (Sasha) Aravkin (UW), Jialu Ran (Emory), Sarah Shultz, David Benkeser, Xiyuan Tan, Xucheng (Fred) Huang, Hely Patel, Jamie Kortanek, Ashante Thompson.

Acknowledgments

We thank Peng Zheng (University of Washington), Kate Revill (FERN Imaging Center at Emory University), Jamie Kortanek, Ashante Thompson, Jennifer Hamel, Hely Patel, Jewel Okoronkwo, Sydney Olson, Sasha Greenspan, Auscia Williams, Malerie McDowell, Cheryl Klaiman, Jose Paredes (Marcus Autism Center), Lei Zhou (Emory University), Tianwen Ma (Emory University), Sijian Fan (University of South Carolina), Deqiang Qiu (Emory University), and Vishwadeep Ahluwalia (Georgia Tech).

All authors were supported by the National Institute of Mental Health of the National Institutes of Health under award number R01 MH129855. The content is solely the responsibility of the authors and does not necessarily represent the official views of the National Institutes of Health.

References I

- G. I. Allen and M. Maletić-Savatić. Sparse non-negative generalized pca with applications to metabolomics. *Bioinformatics*, 27(21):3029–3035, 2011.
- C. F. Beckmann and S. M. Smith. Probabilistic independent component analysis for functional magnetic resonance imaging. *IEEE transactions on medical imaging*, 23(2):137–152, 2004.
- A. J. Bell and T. J. Sejnowski. An information-maximization approach to blind separation and blind deconvolution. *Neural computation*, 7(6):1129–1159, 1995.
- Y. Benjamini and Y. Hochberg. Controlling the false discovery rate: a practical and powerful approach to multiple testing. *Journal of the Royal statistical society: series B (Methodological)*, 57(1):289–300, 1995.
- B. Biswal, M. Mennes, X.-N. Zuo, S. Gohel, C. Kelly, S. M. Smith, C. F. Beckmann, J. S. Adelstein, R. L. Buckner, S. Colcombe, et al. Toward discovery science of human brain function. *Proceedings of the national academy of sciences*, 107(10):4734–4739, 2010.
- Z. Boukouvalas, Y. Levin-Schwartz, V. D. Calhoun, and T. Adali. Sparsity and independence: Balancing two objectives in optimization for source separation with application to fmri analysis. *Journal of the Franklin Institute*, 355(4):1873–1887, 2018.
- V. D. Calhoun, T. Adali, G. D. Pearson, and J. J. Pekar. A method for making group inferences from functional mri data using independent component analysis. *Human brain mapping*, 14(3):140–151, 2001.
- K. T. Cosgrove, T. J. McDermott, E. J. White, M. W. Mosconi, W. K. Thompson, M. P. Paulus, C. Cardenas-Iniguez, and R. L. Aupperle. Limits to the generalizability of resting-state functional magnetic resonance imaging studies of youth: An examination of abcd study® baseline data. *Brain imaging and behavior*, 16(4):1919–1925, 2022.
- B. Deen and K. Pelphrey. Perspective: brain scans need a rethink. *Nature*, 491(7422):S20–S20, 2012.
- A. Di Martino, E. Al, and M. P. Milham. The autism brain imaging data exchange: towards a large-scale evaluation of the intrinsic brain architecture in autism. *Molecular Psychiatry* 2014 19:6, 19(6):659–667, 6 2013. ISSN 1476-5578. doi: 10.1038/mp.2013.78.
- A. Di Martino, C.-G. Yan, Q. Li, E. Denio, F. X. Castellanos, K. Alaerts, J. S. Anderson, M. Assaf, S. Y. Bookheimer, M. Dapretto, et al. The autism brain imaging data exchange: towards a large-scale evaluation of the intrinsic brain architecture in autism. *Molecular psychiatry*, 19(6):659–667, 2014.

References II

- A. Di Martino, D. O'connor, B. Chen, K. Alaerts, J. S. Anderson, M. Assaf, J. H. Balsters, L. Baxter, A. Beggiato, S. Bernaerts, et al. Enhancing studies of the connectome in autism using the autism brain imaging data exchange ii. *Scientific data*, 4(1):1–15, 2017.
- I. Díaz, N. S. Hejazi, K. E. Rudolph, and M. J. van Der Laan. Nonparametric efficient causal mediation with intermediate confounders. *Biometrika*, 108(3):627–641, 2021.
- R. Ge, Y. Wang, J. Zhang, L. Yao, H. Zhang, and Z. Long. Improved fastica algorithm in fmri data analysis using the sparsity property of the sources. *Journal of neuroscience methods*, 263:103–114, 2016.
- N. S. Hejazi, M. J. van der Laan, and D. C. Benkeser. haldensify: Highly adaptive lasso conditional density estimation in R. *Journal of Open Source Software*, 2022. doi: 10.21105/joss.04522. URL <https://doi.org/10.21105/joss.04522>.
- A. Hyvarinen. Fast and robust fixed-point algorithms for independent component analysis. *IEEE transactions on Neural Networks*, 10(3):626–634, 1999.
- M. A. Just, T. A. Keller, V. L. Malave, R. K. Kana, and S. Varma. Autism as a neural systems disorder: a theory of frontal-posterior underconnectivity. *Neuroscience & Biobehavioral Reviews*, 36(4):1292–1313, 2012.
- C. L. Keown, P. Shih, A. Nair, N. Peterson, M. E. Mulvey, and R.-A. Müller. Local functional overconnectivity in posterior brain regions is associated with symptom severity in autism spectrum disorders. *Cell reports*, 5(3):567–572, 2013.
- S. Lee, J. D. Bijsterbosch, F. A. Almagro, L. Elliott, P. McCarthy, B. Taschler, R. Sala-Llonch, C. F. Beckmann, E. P. Duff, S. M. Smith, et al. Amplitudes of resting-state functional networks—investigation into their correlates and biophysical properties. *NeuroImage*, 265:119779, 2023.
- M. V. Lombardo, L. Eyler, A. Moore, M. Datko, C. Carter Barnes, D. Cha, et al. Default mode-visual network hypoconnectivity in an autism subtype with pronounced social visual engagement difficulties. *elife*, 8:e47427, 2019.

References III

- S. Marek, B. Tervo-Clemmens, F. J. Calabro, D. F. Montez, B. P. Kay, A. S. Hatoum, M. R. Donohue, W. Foran, R. L. Miller, T. J. Hendrickson, S. M. Malone, S. Kandala, E. Feczko, O. Miranda-Dominguez, A. M. Graham, E. A. Earl, A. J. Perrone, M. Cordova, O. Doyle, L. A. Moore, G. M. Conan, J. Uriarte, K. Snider, B. J. Lynch, J. C. Wilgenbusch, T. Pengo, A. Tam, J. Chen, D. J. Newbold, A. Zheng, N. A. Seider, A. N. Van, A. Metoki, R. J. Chauvin, T. O. Laumann, D. J. Greene, S. E. Petersen, H. Garavan, W. K. Thompson, T. E. Nichols, B. T. Yeo, D. M. Barch, B. Luna, D. A. Fair, and N. U. Dosenbach. Reproducible brain-wide association studies require thousands of individuals. *Nature* 2022 603:7902, 603(7902):654–660, 3 2022. ISSN 1476-4687. doi: 10.1038/s41586-022-04492-9. URL <https://www.nature.com/articles/s41586-022-04492-9>.
- M. B. Nebel, D. E. Lidstone, L. Wang, D. Benkeser, S. H. Mostofsky, and B. B. Risk. Accounting for motion in resting-state fmri: What part of the spectrum are we characterizing in autism spectrum disorder? *NeuroImage*, 257:119296, 2022.
- A. N. Nielsen, D. J. Greene, C. Gratton, N. U. Dosenbach, S. E. Petersen, and B. L. Schlaggar. Evaluating the prediction of brain maturity from functional connectivity after motion artifact denoising. *Cerebral Cortex*, 29(6):2455–2469, 2019.
- J. D. Power, A. Mitra, T. O. Laumann, A. Z. Snyder, B. L. Schlaggar, and S. E. Petersen. Methods to detect, characterize, and remove motion artifact in resting state fmri. *Neuroimage*, 84:320–341, 2014.
- J. Ran, S. Shultz, B. B. Risk, and D. Benkeser. Nonparametric motion control in functional connectivity studies in children with autism spectrum disorder. *arXiv preprint arXiv:2406.13111*, 2024.
- J. M. Robins. Robust estimation in sequentially ignorable missing data and causal inference models. In *Proceedings of the American Statistical Association*, volume 1999, pages 6–10. Indianapolis, IN, 2000.
- J. M. Robins, A. Rotnitzky, and L. P. Zhao. Estimation of regression coefficients when some regressors are not always observed. *Journal of the American statistical Association*, 89(427):846–866, 1994.
- T. D. Satterthwaite, D. H. Wolf, J. Loughead, K. Ruparel, M. A. Elliott, H. Hakonarson, R. C. Gur, and R. E. Gur. Impact of in-scanner head motion on multiple measures of functional connectivity: relevance for studies of neurodevelopment in youth. *Neuroimage*, 60(1):623–632, 2012.
- K. Shaw, S. Williams, M. Patrick, and et al. Prevalence and early identification of autism spectrum disorder among children aged 4 and 8 years—autism and developmental disabilities monitoring network, 16 sites, united states, 2022. *MMWR Surveillance Summaries*, 74, 2025.

References IV

- H. Shen and J. Z. Huang. Sparse principal component analysis via regularized low rank matrix approximation. *Journal of multivariate analysis*, 99(6):1015–1034, 2008.
- S. M. Smith, P. T. Fox, K. L. Miller, D. C. Glahn, P. M. Fox, C. E. Mackay, N. Filippini, K. E. Watkins, R. Toro, A. R. Laird, et al. Correspondence of the brain's functional architecture during activation and rest. *Proceedings of the national academy of sciences*, 106(31):13040–13045, 2009.
- S. M. Smith, T. E. Nichols, D. Vidaurre, A. M. Winkler, T. E. Behrens, et al. A positive-negative mode of population covariation links brain connectivity, demographics and behavior. *Nature neuroscience*, 18(11):1565–1567, 2015.
- B. E. Yerys, E. M. Gordon, D. N. Abrams, T. D. Satterthwaite, R. Weinblatt, K. F. Jankowski, J. Strang, L. Kenworthy, W. D. Gaillard, and C. J. Vaidya. Default mode network segregation and social deficits in autism spectrum disorder: Evidence from non-medicated children. *NeuroImage: Clinical*, 9:223–232, 2015.
- P. Zheng and A. Aravkin. Relax-and-split method for nonconvex inverse problems. *Inverse Problems*, 36(9):095013, 2020.
- H. Zou, T. Hastie, and R. Tibshirani. Sparse principal component analysis. *Journal of computational and graphical statistics*, 15(2):265–286, 2006.

MoCo Absolute Continuity Assumption

$$\int \left[\left\{ \mu_{Y|A,M,X,Z}(1, m, x, z) p_{Z|A,X}(z|1, x) \right. \right. \\ \left. \left. - \mu_{Y|A,M,X,Z}(0, m, x, z) p_{Z|A,X}(z|0, x) \right\} \right. \\ \left. p_{M|\Delta=1,A,X}(m|0, x) p_X(x) \right] dz dm dx .$$

Assumption (Common support (positivity))

Let $P(B)$ be the probability measure of $\{Y, A, M, X, Z\}$ on some set B . Let $P^*(B)$ be the measure corresponding to the joint density $p_{Y|A,M,X,Z}(y|a, m, x, z) p_{Z|A,X}(z|a, x) p_{M|\Delta=1,A,X}(m|0, x) p_X(x)$.

We assume $P^* \ll P$.

$P^*(B) > 0 \implies P(B) > 0$ ensures that it is possible to observe functional connectivity Y in the ASD group across combinations of tolerable motion levels M and more severe symptomatology Z .

Identification

Theorem (Identifiability)

Under the following assumptions:

- (A1) *No missing confounders: $E_C\{Y(m) | A = a, X, Z\} = E_C\{Y(m) | A = a, M = m, X, Z\}$;*
- (A2) *Positivity:*
 - (A2.1) *for every x such that $p_X(x) > 0$, we also have $p_{a|X}(x) > 0$ for $a = 0, 1$;*
 - (A2.2) *for every (x, z, m) such that $p_X(x)p_{Z|a,X}(z | x)p_{M|\Delta=1,0,X}(m | x) > 0$, we also have that $p_{M|a,X,Z}(m | x, z) > 0$ for $a = 0, 1$.*
- (A3) *Causal Consistency: for any child with observed motion value $M = m$, the observed functional connectivity measurement Y is equal to the counterfactual functional connectivity measurement $Y(m)$.*

The counterfactual $\theta_{C,a}$ is identified by θ_a , where

$$\theta_1 = \iiint \mu_{Y|1,M,X,Z}(m, x, z) p_{Z|1,X}(z | x) p_{M|\Delta=1,0,X}(m | x) p_X(x) dz dm dx$$

$$\theta_0 = \iiint \mu_{Y|0,M,X,Z}(m, x, z) p_{Z|0,X}(z | x) p_{M|\Delta=1,0,X}(m | x) p_X(x) dz dm dx$$

Estimation, 1/3

1. *Estimate mean functional connectivity* $\mu_{Y|A,M,X,Z}$. Fit a super learner regression using Y as the outcome and including A , M , X , and Z as predictors. Evaluate the fitted value for $i = 1, \dots, n$ and for $a = 0, 1$.
2. *Estimate motion distributions* $p_{M|A,X}$, $p_{M|\Delta=1,A,X}$, $p_{M|A,X,Z}$, and $p_{M|\Delta=1,A,X,Z}$. Estimate densities using the highly adaptive LASSO and evaluate for $a = 0, 1$ and $i = 1, \dots, n$.
3. *Estimate motion-standardized functional connectivity* $\eta_{\mu|A,Z,X}$. Create the pseudo-outcome
$$\hat{Y}_{M,i} = \mu_{n,Y|A,M,X,Z}(A_i, M_i, X_i, Z_i) \times \frac{p_{n,M|\Delta=1,A,X}(M_i|0, X_i)}{p_{n,M|\Delta=1,A,X,Z}(M_i|A_i, X_i, Z_i)}.$$
 Using only observations with $\Delta_i = 1$, fit a super learner regression using \hat{Y}_M as the outcome and A , Z , and X as predictors. Set A to a evaluate for $i = 1, \dots, n$.

Estimation, 2/3

4. Estimate Z-standardized functional connectivity $\eta_{\mu|A,M,X}$. Create the pseudo-outcome

$\hat{Y}_{Z,i} = \mu_{n,Y|A,M,X,Z}(A_i, M_i, X_i, Z_i) \times \frac{p_{n,M|A,X}(M_i|A_i, X_i)}{p_{n,M|A,X,Z}(M_i|A_i, X_i, Z_i)}$. Fit a super learner regression using \hat{Y}_Z as the outcome and including M , X , and A as predictors. Set A to a and evaluate for $i = 1, \dots, n$.

5. Estimate motion- and Z-standardized functional connectivity $\xi_{a,\eta|X}$. Fit a super learner regression using $\eta_{n,\mu|A,Z,X}$ as the outcome and including A and X as predictors. For $a = 0, 1$, evaluate the fitted value for $i = 1, \dots, n$.

6. Calculate plug-in estimate. Compute the plug-in estimate $\theta_{n,a} = n^{-1} \sum_{i=1}^n \xi_{n,a,\eta|X}(X_i)$.

Estimation, 3/3

7. Estimate propensities.

i. *Estimate diagnosis distribution π_a* Fit a super learner regression using A as the outcome and including X as predictors. Evaluate for $i = 1, \dots, n$ and set $\pi_{n,0}(X_i) = 1 - \pi_{n,1}(X_i)$.

ii. *Estimate inclusion probability $\pi_{\Delta=1|A,X}$* . Fit a super learner using Δ as the outcome and including A and X as predictors. Set A to 0 to obtain $\pi_{n,\Delta=1|A,X}(0, X_i)$ for $i = 1, \dots, n$. Compute

$$\bar{\pi}_{n,0}(X_i) = \pi_{n,0}(X_i)\pi_{n,\Delta=1|A,X}(0, X_i) \text{ for } i = 1, \dots, n.$$

8. *Evaluate estimated efficient influence function $D_{n,a}(O_i)$* . For $a = 0, 1$ and each $i = 1, \dots, n$, evaluate $D_{n,a}(O_i)$ by substituting the fitted values based on the estimated nuisance parameters obtained in steps 1-7 into the influence function equation.

9. *Compute the one-step estimator*. For $a = 0, 1$, compute

$$\theta_{n,a}^+ = \theta_{n,a} + n^{-1} \sum_{i=1}^n D_{n,a}(O_i).$$

Simulation: Confirming theoretical properties of estimators

Case I: all nuisance parameters are consistently estimated at appropriate rates

n	$\theta_{n,0}^{\text{cf}}$				$\theta_{n,1}^{\text{cf}}$			
	$n^{1/2}$ bias	$n^{1/2}$ sd	sd ratio	cover	$n^{1/2}$ bias	$n^{1/2}$ sd	sd ratio	cover
200	-0.235	2.063	1.075	0.929	-0.246	2.358	1.430	0.851
500	-0.150	1.938	0.986	0.951	-0.310	2.369	1.205	0.900
1000	-0.141	2.003	1.028	0.940	-0.113	2.333	1.110	0.922
2000	-0.026	1.977	1.033	0.940	-0.077	2.328	1.056	0.931
4000	-0.006	1.913	1.014	0.950	0.076	2.074	0.914	0.979

Table: All nuisance parameters are consistently estimated at appropriate rates with the use of cross-fitting